

Enhanced Dichroism of Polarizing Composite Films by Embedding Sepiolite

So Yeon Ahn and Young Seok Song*

Cite This: *ACS Omega* 2024, 9, 25793–25799

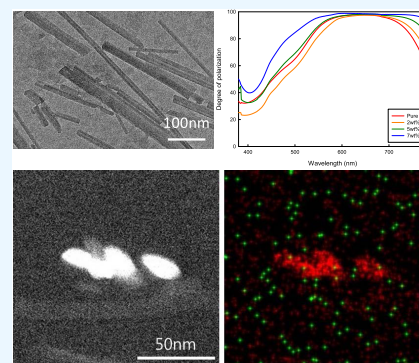
Read Online

ACCESS |

Metrics & More

Article Recommendations

ABSTRACT: The present study investigated the use of fibrous nanoparticle-filled polarizing films. Sepiolites were selected as nanoparticles and incorporated into a PVA–iodine complex. The resulting nanocomposite film was elongated and dyed with iodine. Various properties of the nanocomposite polarizing films, including thermal, morphological, optical, and rheological features, were experimentally analyzed. The study demonstrated that an increase in sepiolite loading was accompanied by an enhancement in both the mechanical and viscoelastic properties. In particular, the incorporation of nanoparticles led to an increase in birefringence and the degree of polarization. This was attributed to the alteration of the internal structure of the PVA film caused by the embedded sepiolites. The thermal analysis showed that the composite film with a higher content of sepiolites exhibited higher crystallinity and a higher melting temperature.



1. INTRODUCTION

Currently, poly(vinyl alcohol) (PVA)-based polarizing films are extensively employed in various display applications due to their dichroic feature.^{1–4} The fabrication of these films typically involves several unit processes. The initial stage of the fabrication process involves swelling in an aqueous solution followed by immersion in a solution containing iodine and potassium iodide for iodine adsorption. Subsequently, the films are elongated to achieve a high degree of uniaxial orientation. This process results in the formation of blue complexes between adsorbed iodine and PVA molecules, which are aligned in the direction of elongation. This leads to a remarkable increase in polarizability.⁵ In comparison to other polymeric polarizers, the PVA–iodine complex exhibits several advantages, including high transmittance, superior alignment, and cost-effectiveness in production.⁶ However, commercially available polarizing films exhibit certain inherent limitations. These include low thermal stability, susceptibility to iodine desorption, poor water stability, high residual stress, and limited mechanical surface properties.⁷ To address these shortcomings, a multitude of studies have been conducted. For instance, the replacement of common atactic PVA with highly syndiotactic PVA has been considered as a potential solution to the aforementioned issues. However, this approach has been met with challenges, including increased costs and relatively lower iodine adsorption.^{8–10}

To date, the majority of research on clay-filled composites has primarily utilized natural layered silicate clays, such as montmorillonite (MMT).^{11–14} In most instances, these fillers have served as reinforcing agents in polymeric matrices, yet

significant advancements in the field remain elusive. On the other hand, sepiolite emerges as a promising material with applications spanning a wide spectrum due to its sorptive, rheological, and catalytic properties.^{15–18} While sepiolite is a member of the clay family, it exhibits a fibrous characteristic that is distinct from that of conventional plate-like particles. The structure of this material is composed of two tetrahedral silica sheets and a central octahedral sheet with magnesium. These blocks assemble into ribbons with an open tunnel that is capable of accommodating water and exchange ions.¹⁹ It has also been reported that the specific surface area of sepiolites is lower for a given aspect ratio than that of layer-structured silicates. This implies that sepiolite may exhibit greater interactions between particles and matrix than other materials.²⁰ For this reason, sepiolite is shown to be useful in various applications, such as environmental deodorants, catalyst carriers, paints, decolorizing agents, plastisols, detergents, and thickeners.²¹

The objective of this study is to investigate the dichroic characteristics of sepiolite-embedded polarizing films. Sepiolites were incorporated into the PVA matrix, and the resulting composite film was elongated in an iodine solution. A series of analyses were conducted to gain insights into the physical

Received: December 27, 2023

Revised: May 19, 2024

Accepted: May 28, 2024

Published: June 6, 2024



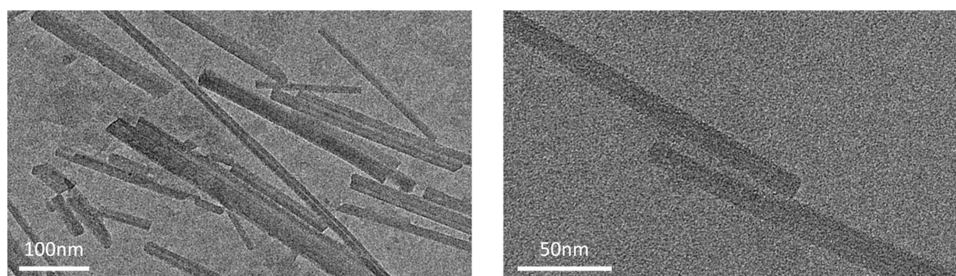


Figure 1. TEM images of the sepiolites.

behavior of dichroic nanocomposite films, encompassing morphological, optical, mechanical, and rheological experiments. Moreover, the impact of varying the sepiolite loading was evaluated by contrasting it with that of pure PVA polarizers.

2. EXPERIMENTAL SECTION

2.1. Materials and Sample Preparation. Sepiolite ($\text{Mg}_2\text{H}_2(\text{SiO}_3)_3 \cdot x\text{H}_2\text{O}$) was supplied by Sigma-Aldrich, and its average length was $1 \mu\text{m}$. Poly(vinyl alcohol) (PVA) with a molecular weight of 85,000–124,000 was bought from Sigma-Aldrich. Iodine and potassium iodide were obtained from Iodeal Brands Co., and boric acid was purchased from Quiborax Co. All materials were used as received. To prepare sepiolite-filled PVA films, PVA was dissolved at $80 \text{ }^\circ\text{C}$ for 4 h, and the clay particles were added to the solution. Sonication was also applied to the suspension for 30 min. The particle suspension was cast and dried in a Petri dish. The film was kept in an I_2/KI solution of 0.4 wt % at $30 \text{ }^\circ\text{C}$ for 5 min and drawn two times in a 5 wt % boric acid solution at $50 \text{ }^\circ\text{C}$.

2.2. Measurements. Morphological analysis of the sepiolites was carried out with a transmission electron microscope (TEM, JEM-200CX (JEOL)). A 200-mesh TEM grid was utilized, and a voltage of 200 kV was imposed. The composition of the specimens was evaluated with an EDAX Genesis XM4 system. In addition, cross-sectional images of the samples were analyzed with a field emission scanning electron microscope (FE-SEM, S-4300, Veeco). Before the observation, all specimens were coated with platinum using an ion sputter coater (JEOL, JFC-1100E).

Single transmittance of the samples was measured at a wavelength range of 300–800 nm using a UV–visible spectrometer (Lambda 25, PerkinElmer). In the case where the transition dipole moment is directed along the long axis of the molecules, the dichroic ratio R and the order parameter S are respectively defined as

$$R = \frac{A_{\parallel}}{A_{\perp}} \quad (1)$$

$$S = \frac{R - 1}{R + 2} \quad (2)$$

where A_{\parallel} and A_{\perp} denote the absorbance parallel and perpendicular to the average orientation of the long axis of the chromophores, respectively. The degree of polarization (DP), a measure of the extent to which the light is polarized, was computed as follows²²

$$\text{DP} (\%) = \frac{T_{\max} - T_{\min}}{T_{\max} + T_{\min}} \times 100 \quad (3)$$

where T_{\max} and T_{\min} are the minimum and maximum transmittances of light, respectively. Birefringence of the composite films was measured with a Leitz orthoplanar polarizing microscope (Leica, Germany). Retardation of the PVA films was determined with a B-type Berek compensator. The thickness of the samples was 30–75 μm . The birefringence was calculated using the following equation

$$\Gamma = \Delta n \times d \quad (4)$$

where Γ is the retardation, Δn is the birefringence, and d is the sample thickness. Rheological characteristics of the films were evaluated by using a rheometer (MCR 302, Anton Paar) equipped with a cone and plate fixture. The steady shear viscosity was measured in the shear rate range from 0.01 to 1000 s^{-1} . Prior to the test, the previous shear stress history was removed. In the oscillatory shear mode, dynamic viscoelastic properties, including the storage modulus, loss modulus, and complex viscosity, were measured by applying an angular frequency sweep of $0.1\text{--}100 \text{ rad}\cdot\text{s}^{-1}$. The applied strain was 0.1% during the oscillatory shear test. All rheological measurements were conducted at $30 \text{ }^\circ\text{C}$ unless otherwise stated. In addition, dynamic mechanical analysis (DMA) for the composite film was conducted using a universal extensional fixture UXF kit (Anton Paar). Two different experimental conditions were considered. First, angular frequencies of $1\text{--}30 \text{ rad}\cdot\text{s}^{-1}$ were swept at a constant temperature of $30 \text{ }^\circ\text{C}$. The applied temperature sweep was from 60 to $150 \text{ }^\circ\text{C}$ at a constant frequency of 1 Hz. The measurement chamber was purged with N_2 during the heating. Thermal characteristics of the specimens were investigated using differential scanning calorimetry (DSC, Q2000 system, TA Instruments). The specimens for the DSC experiments were scanned from 30 to $300 \text{ }^\circ\text{C}$ at $10 \text{ }^\circ\text{C}/\text{min}$. Mechanical properties such as tensile strength, Young's modulus, and elongation at break were evaluated using a universal testing machine (UTM, Instron 3365) according to ASTM D638. The film specimens with a thickness of $0.2 \mu\text{m}$ were prepared, and an elongation rate of 5 mm/min was applied.

3. RESULTS AND DISCUSSION

Figure 1 shows the TEM images of the sepiolites used in this study. The fibrous particles were found to have a diameter of 10–30 nm, which implies that their aspect ratios are in the range from 30 to 100. When the nanofibrous sepiolites were incorporated into PVA, the composite films were quite transparent.

Figure 2 presents the steady shear viscosities of the sepiolites suspended in aqueous solutions. It was found that the viscosities decreased with increasing shear rate. This is the well-known shear thinning behavior. The applied shear stress causes the sepiolite nanofibers to be oriented along the shear

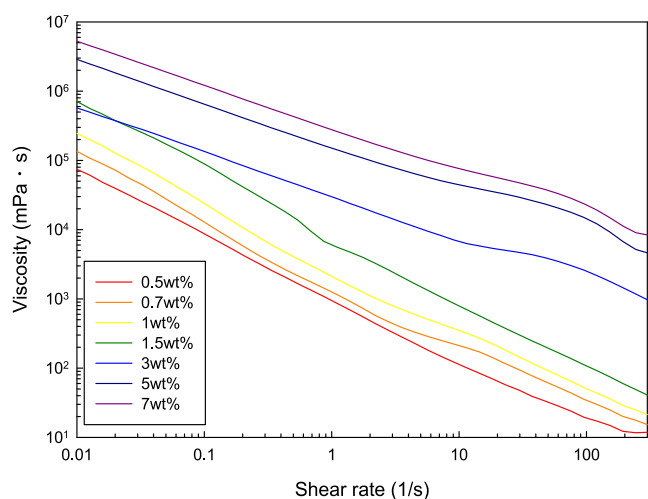


Figure 2. Steady shear viscosity as a function of shear rate.

flow direction. Consequently, the hydrodynamic flow resistance decreases. Meanwhile, the content of the sepiolites had a remarkable effect on the shear viscosities. That is, as the fiber loading increased, the resulting shear viscosities increased significantly. In particular, the sepiolite suspensions containing a relatively higher concentration of the particles showed a low slope in the high shear rate region. This means a low power law index when considering the power law model, $\tau = K\dot{\gamma}^n$, where K is the flow consistency index and n is the power law index.

Viscoelastic material functions can be used for non-destructive analysis. In the current study, we adopted the oscillatory shear rheological experiment as one of the analyzing methods. Figure 3 presents the material functions, i.e., storage modulus, loss modulus, and complex viscosity, as a function of angular frequency. The storage and loss moduli increased by increasing the loading of the particles. However, their slopes did not change with respect to the filler content. Similar to the simple shear results, the complex viscosities decreased as a function of angular frequency. According to the Cox–Merz rule, the magnitude of complex viscosity is equal to that of shear viscosity at the corresponding values of angular frequency and shear rate, i.e., $\eta(\dot{\gamma}) = |\eta^*|_{\omega=\dot{\gamma}}$. Here, $\eta^*(\omega) = \eta'(\omega) - i\eta''(\omega)$ is the complex viscosity.²³ In general, the complex viscosity measured at high angular frequencies is more stable than the shear viscosity at high shear rates. The suspension prepared in this study was found not to obey the Cox–Merz rule.

In addition to the oscillatory shear test, DMA experiments were carried out to further investigate the viscoelastic behavior of the composite film in the extension mode. For the DMA test, a sinusoidal stress is applied to samples, and the resulting strain is measured at time t . Consequently, a phase lag occurs during the test as follows

$$\sigma(t) = \sigma_0 \sin(\omega t + \delta) \quad (5)$$

$$\varepsilon(t) = \varepsilon_0 \sin \omega t \quad (6)$$

where δ denotes a phase lag between the stress and the strain. The storage modulus (E') and the loss modulus (E'') are defined by $E' = \sigma_0/\varepsilon_0 \cos \delta$ and $E'' = \sigma_0/\varepsilon_0 \sin \delta$, respectively.

Figure 4 presents the DMA results of the samples. The addition of more sepiolites led to a higher storage modulus (Figure 4a) and a lower loss factor (Figure 4b). As the temperature increased, the storage modulus decreased. It has

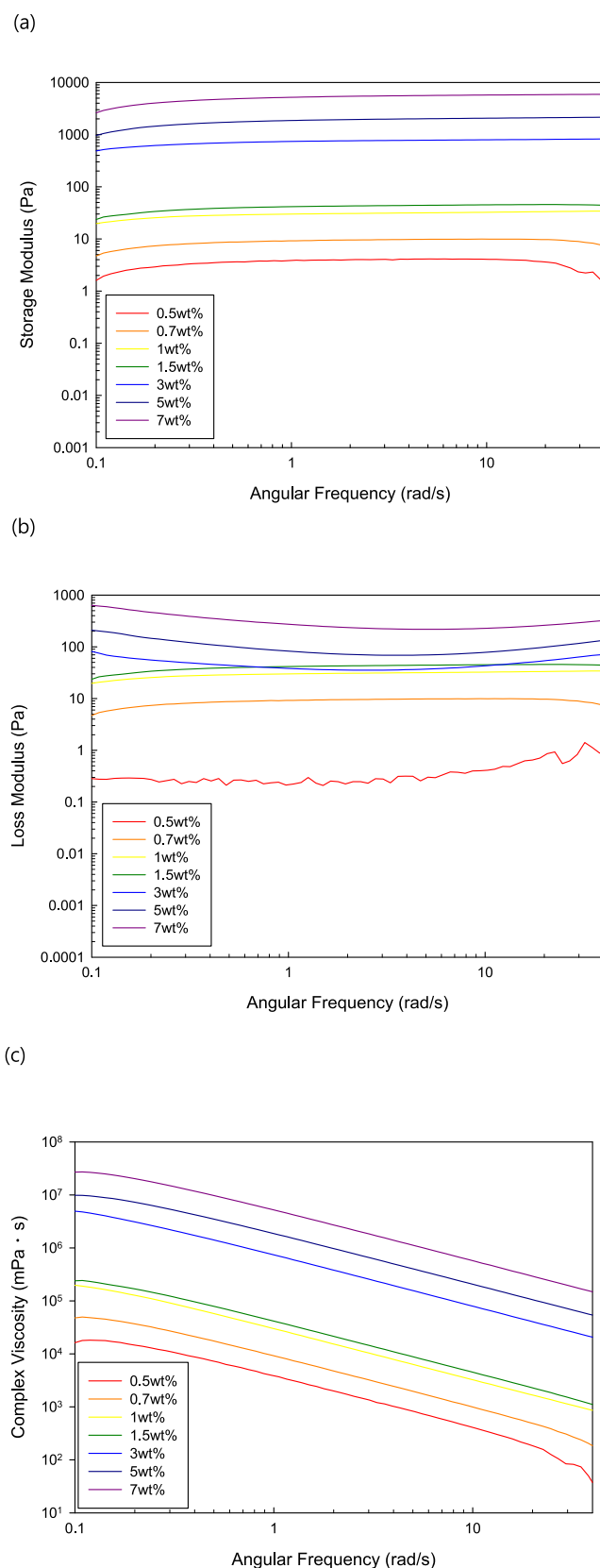


Figure 3. Viscoelastic functions: (a) storage modulus, (b) loss modulus, and (c) complex viscosity of the sepiolite suspension as a function of angular frequency.

been reported that the peak temperatures of the loss factor (or the loss modulus) are associated with a glass transition of

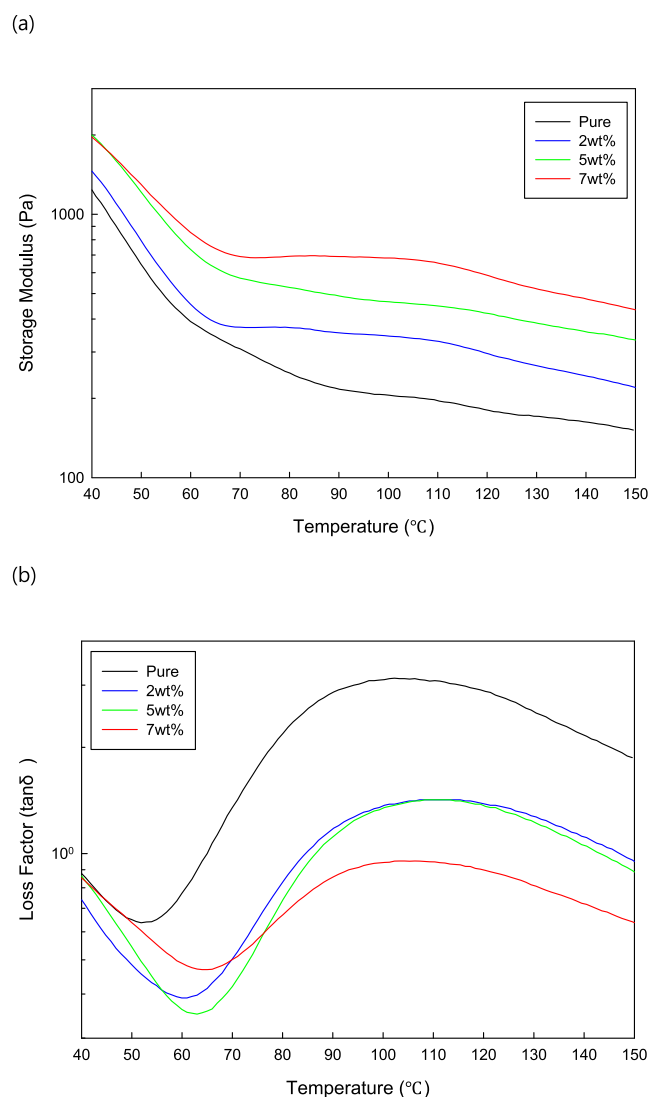


Figure 4. DMA results: (a) storage modulus and (b) loss factor as a function of temperature.

polymers. Figure 4b shows that the peak temperatures of the loss factor were shifted toward the right side with respect to the particle content.

Figure 5a,b displays photographs of the pure PVA film and the composite film with a 7% particle loading. Considering the elemental composition of sepiolites (i.e., Mg, Si, H, and O) and the chemical structure (i.e., $\text{Mg}_2\text{H}_2(\text{SiO}_3)_3 \cdot x\text{H}_2\text{O}$), the nanoparticles possess a hydrophilic feature. Therefore, they can be well-dispersed in an aqueous solution. That is why the nanoparticle-incorporated film showed a fairly good transparency, which will be further explained later. When the film was elongated 2-fold, not only the PVA molecules but also the nanofibers were oriented along the elongation direction. As a result, birefringence was developed in the film. Figure 5c presents the birefringence image of the specimen. The interference colors were observed when the composite film was placed between two crossed polarizing films. When linearly polarized light passes through the film with anisotropic refractive indices, it is split into slow and fast lights, thus leading to a phase difference in the light. After that, the light travels through the rear polarizer and interferes destructively or constructively, depending on the phase difference.

Figure 6 demonstrates the birefringence results of the samples. The birefringence was found to increase with increasing loading of the nanofibers. When the film was elongated, the PVA molecules and fibrous nanoparticles were oriented as a result. Since the sepiolites have anisotropic refractive indices, i.e., 1.53 and 1.52 in the longitudinal and transverse directions, respectively, the birefringence feature can be strengthened with respect to the particle loading. Also, the addition of the sepiolites can help the PVA molecules to be aligned in the extension direction. The birefringence results show the potential of using the sepiolites embedded in the PVA film as an optical element such as a wave plate. In particular, the composite film with a particle content of 7 wt % showed a significantly enhanced birefringence value compared with that of the pure PVA film.

Figure 7 presents the cross-sectional SEM images of the composite films. The specimens were stretched and dyed with iodine. The images showed that the sepiolite-embedded films

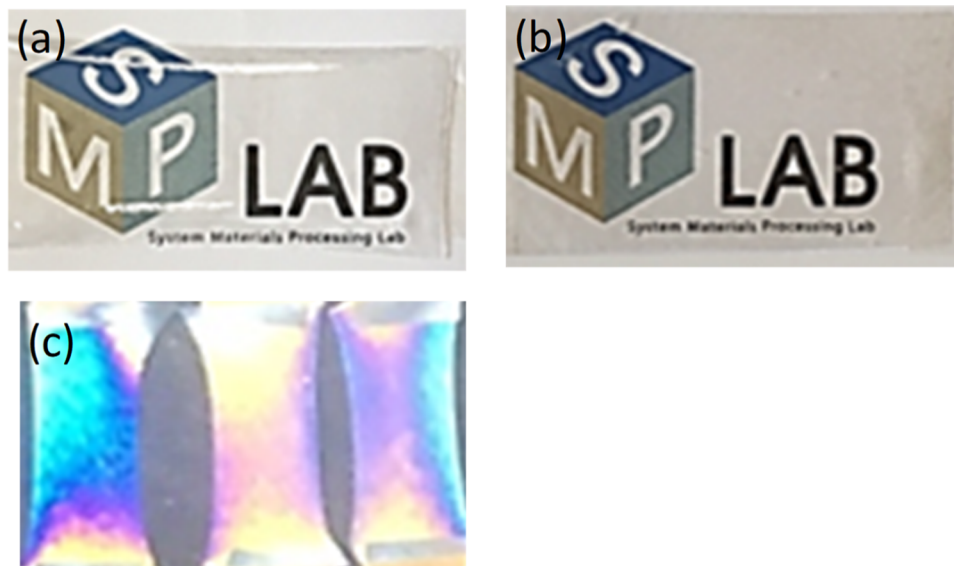


Figure 5. Photo images of (a) pure PVA film and (b) 7 wt % sepiolite-embedded PVA film. (c) Birefringence images of the stretched films.

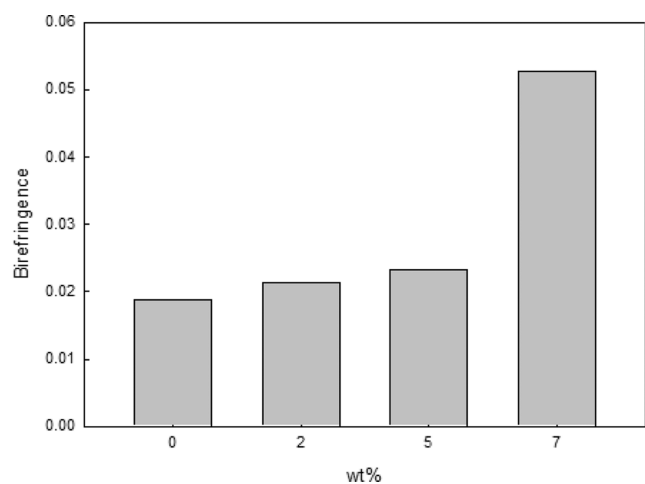


Figure 6. Birefringence of the composite films with respect to the sepiolite content.

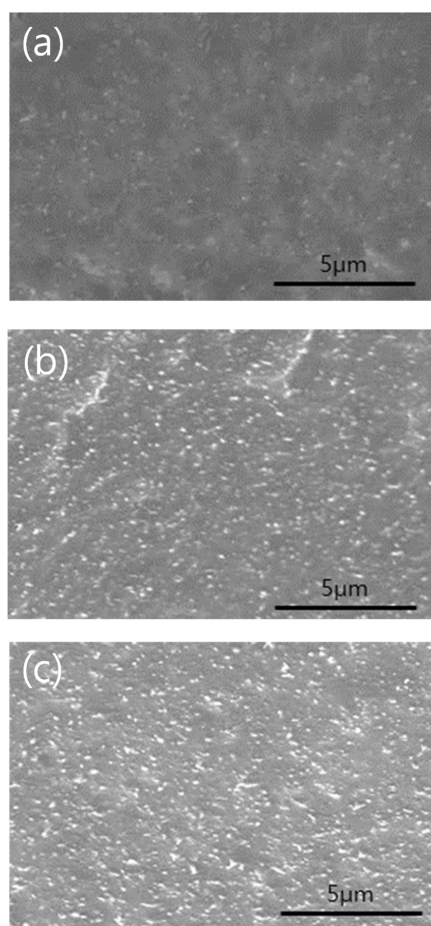


Figure 7. FE-SEM images of the cross sections: (a) 2 wt %, (b) 5 wt %, and (c) 7 wt % sepiolite loadings.

had a good dispersion of the nanofibers in the matrix, and the sepiolites were aligned along the stretching direction of the film. As the filler loading increased, the particle density detected on the cross-section increased. Also, the so-called pull-out phenomenon was not observed in the images, which implied that the nanofibers had kind of good interfacial bonding strength to the matrix.

It has been reported that the content and structure of iodine in the PVA play key roles in determining the degree of polarization for the film. Therefore, it is meaningful to look into the configurations of the iodine and sepiolites in the PVA matrix. Figure 8a demonstrates the TEM images of the iodine-

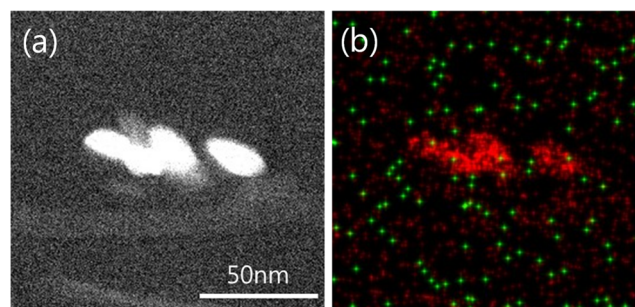


Figure 8. (a) TEM and (b) EDAX images of the iodine-dyed composite film. The red represents silicon, and the green indicates iodine.

dyed sepiolite/PVA film. In the image, white dots denote the sepiolite. The EDAX image is presented in Figure 8b. The green and red dots indicate the elements silicon and iodine, respectively. It turned out that a relatively large amount of iodine was detected around the sepiolites, thus leading to the enhancement of iodine sorption. One reason for this may be a change in the internal structure of the PVA, i.e., the crystal structure of the matrix. It is known that PVA and iodine form a complex structure and conformation in a polarizing film.^{4,5} In particular, crystal structures such as helical and aggregate model-based structures have been assumed to account for the polarization behavior of the dyed film. The helical model presumes that a polyiodine is surrounded by PVA chains along the spiral axis. In the aggregate model, I_3^- or I_3^- are situated between the planar zigzag PVA chains. When the concentration of iodine is high enough, the PVA–iodine complex forms in the crystal phase and iodine molecules are physically adsorbed in the amorphous phase of PVA. Figure 9 shows the DSC results of the specimens. When the sepiolites were incorporated into the PVA matrix, the creation of the crystal structure was facilitated. This is because the sepiolite can act as a nucleation site in the matrix. Consequently, the iodine sorption increased when the sepiolites were embedded into the PVA. The change of the crystallinity with respect to the sepiolite content is presented in Figure 9a. As the nanofiber loading increased, the resulting crystallinity increased. Figure 9b shows the melting temperatures of the composite films. In general, the higher crystallinity of the polymer yields a higher melting temperature. As expected, the sample with a 7 wt % content of the sepiolites was found to have the highest melting temperature.

The mechanical characteristics of the samples are illustrated in Figure 10. It was found that Young's modulus increased with increasing weight percent of the sepiolites, especially at 7 wt % loading of the particles. On the contrary, the elongation at break decreased with an increase in the particle loading. Interestingly, the sudden enhancement in the modulus was similar to the birefringence result. We inferred that the microstructure of the composite film at a nanofiber loading of 7 wt % changed dramatically.

Figure 11 shows the transmittance and degree of polarization of the sepiolite-embedded films. Please keep in mind

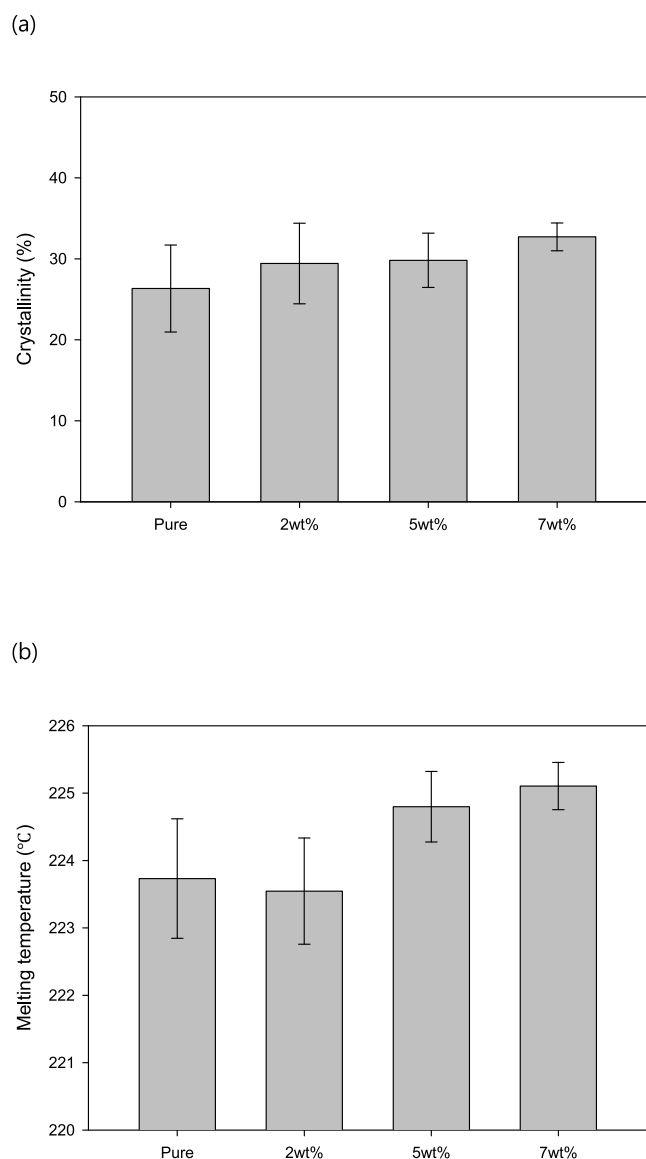


Figure 9. DSC results of the samples: (a) melting temperature and (b) crystallinity as a function of sepiolite loading.

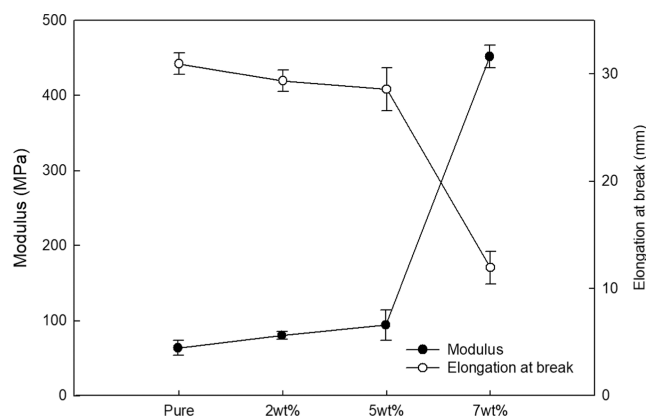


Figure 10. Young's modulus and elongation at break of the samples.

that this study employed a relatively low iodine treatment time (i.e., 5 min) and a low extension ratio of the film (i.e., two times) compared with the general production condition of commercial PVA films. As the content of the sepiolites

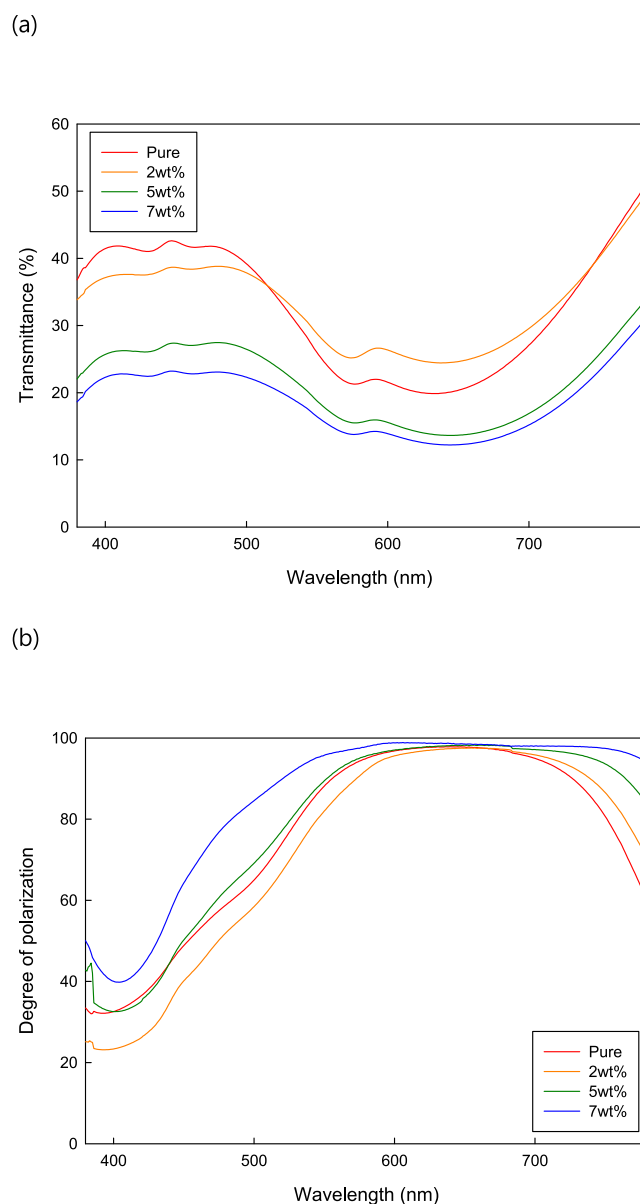


Figure 11. (a) Transmittance and (b) degree of polarization of the prepared sepiolite/PVA polarizing films.

increased, the transmittance of the films decreased drastically. However, the degree of polarization was remarkably improved with increasing the particle content. In particular, compared with the result of pure PVA, the 7 wt % sepiolite-embedded PVA film showed a considerably high degree of polarization.

4. CONCLUSIONS

In the current study, fibrous nanoparticle-embedded PVA films were investigated. To improve the optical features of polarizing films, we employed sepiolites as a nanofiller in the film. The sepiolites were incorporated into the PVA–iodine complex. The prepared composite films were evaluated through morphological, rheological, optical, and mechanical analyses. The results revealed that the sepiolites were well-dispersed in the matrix, and the addition of the sepiolites led to an increase in the mechanical and optical properties. In particular, compared with the pure PVA polarizing film, the nanocomposite film with a filler content of 7 wt % had an

outstanding degree of polarization. Overall, we foresee that embedding sepiolites into a polymer can open a fascinating pathway for developing new optical devices with high performance.

AUTHOR INFORMATION

Corresponding Author

Young Seok Song – Department of Fiber System Engineering, Dankook University, Yongin-si, Gyeonggi-do 448-701, Korea; orcid.org/0000-0002-4462-1605; Phone: +82-31-8005-3567; Email: ysong@dankook.ac.kr; Fax: +82-31-8005-2209

Author

So Yeon Ahn – Department of Fiber System Engineering, Dankook University, Yongin-si, Gyeonggi-do 448-701, Korea

Complete contact information is available at:

<https://pubs.acs.org/10.1021/acsomega.3c10402>

Notes

The authors declare no competing financial interest.

ACKNOWLEDGMENTS

This research was supported by Basic Science Research Program through the National Research Foundation of Korea (NRF) funded by the Korean government (MSIT, No. NRF-2018R1A5A1024127).

REFERENCES

- (1) Miyazaki, T.; Hoshiko, A.; Akasaka, M.; Sakai, M.; Takeda, Y.; Sakurai, S. Structure Model of a Poly(vinyl alcohol) Film Uniaxially Stretched in Water and the Role of Crystallites on the Stress–Strain Relationship. *Macromolecules* **2007**, *40* (23), 8277–8284.
- (2) Choi, Y.-S.; Miyasaka, K. X-Ray Study on the Structure of the Poly(vinyl alcohol)-Iodine Complex. *Polym. J.* **1991**, *23* (8), 977–981.
- (3) Lagerwall, J. P. F.; Schutz, C.; Salajkova, M.; Noh, J.; Hyun Park, J.; Scalia, G.; Bergstrom, L. Cellulose nanocrystal-based materials: from liquid crystal self-assembly and glass formation to multifunctional thin films. *NPG Asia Mater.* **2014**, *6*, No. e80.
- (4) Tashiro, K.; Kitai, H.; Saharin, S. M.; Shimazu, A.; Itou, T. Quantitative Crystal Structure Analysis of Poly(vinyl Alcohol)–Iodine Complexes on the Basis of 2D X-ray Diffraction, Raman Spectra, and Computer Simulation Techniques. *Macromolecules* **2015**, *48* (7), 2138–2148.
- (5) Kim, G. H.; Yoon, K. J. Preparation and properties of polarizing films for liquid crystal display prepared using iodine vapor. *Fibers Polym.* **2013**, *14* (12), 1999–2005.
- (6) Hodge, R. M.; Edward, G. H.; Simon, G. P. Water absorption and states of water in semicrystalline poly(vinyl alcohol) films. *Polymer* **1996**, *37* (8), 1371–1376.
- (7) Kaneko, Y.; Matsuda, S.-i.; Kadokawa, J.-i. Chemoenzymatic synthesis of amylose-grafted poly(vinyl alcohol). *Polym. Chem.* **2010**, *1* (2), 193–197.
- (8) Shin, E. J.; Lyoo, W. S.; Lee, Y. H. Polarizer effect and structure of iodinated before and after casting poly(vinyl alcohol) film. *J. Appl. Polym. Sci.* **2011**, *120* (1), 397–405.
- (9) Yang, H.; Horii, F. Investigation of the structure of poly(vinyl alcohol)–iodine complex hydrogels prepared from the concentrated polymer solutions. *Polymer* **2008**, *49* (3), 785–791.
- (10) Zhang, Q.; Zhang, R.; Meng, L.; Ji, Y.; Su, F.; Lin, Y.; Li, X.; Chen, X.; Lv, F.; Li, L. Stretch-induced structural evolution of poly(vinyl alcohol) film in water at different temperatures: An in-situ synchrotron radiation small- and wide-angle X-ray scattering study. *Polymer* **2018**, *142*, 233–243.
- (11) Manias, E.; Touny, A.; Wu, L.; Strawhecker, K.; Lu, B.; Chung, T. C. Polypropylene/Montmorillonite Nanocomposites. Review of the Synthetic Routes and Materials Properties. *Chem. Mater.* **2001**, *13* (10), 3516–3523.
- (12) Strawhecker, K. E.; Manias, E. Structure and Properties of Poly(vinyl alcohol)/Na⁺ Montmorillonite Nanocomposites. *Chem. Mater.* **2000**, *12* (10), 2943–2949.
- (13) Gorrasi, G.; Tortora, M.; Vittoria, V.; Pollet, E.; Lepoittevin, B.; Alexandre, M.; Dubois, P. Vapor barrier properties of polycaprolactone montmorillonite nanocomposites: effect of clay dispersion. *Polymer* **2003**, *44* (8), 2271–2279.
- (14) Pluta, M.; Galeski, A.; Alexandre, M.; Paul, M.-A.; Dubois, P. Polylactide/montmorillonite nanocomposites and microcomposites prepared by melt blending: Structure and some physical properties. *J. Appl. Polym. Sci.* **2002**, *86* (6), 1497–1506.
- (15) Pratap Singh, V.; Kapur, G. S.; Shashikant; Choudhary, V. High-density polyethylene/needle-like sepiolite clay nanocomposites: effect of functionalized polymers on the dispersion of nanofiller, melt extensional and mechanical properties. *RSC Adv.* **2016**, *6* (64), 59762–59774.
- (16) Nehra, R.; Maiti, S. N.; Jacob, J. Poly(lactic acid)/(styrene-ethylene-butylene-styrene)-g-maleic anhydride copolymer/sepiolite nanocomposites: Investigation of thermo-mechanical and morphological properties. *Polym. Adv. Technol.* **2018**, *29* (1), 234–243.
- (17) Wicklein, B.; Aranda, P.; Ruiz-Hitzky, E.; Darder, M. Hierarchically structured bioactive foams based on polyvinyl alcohol–sepiolite nanocomposites. *J. Mater. Chem. B* **2013**, *1* (23), 2911–2920.
- (18) Ajmal, A. W.; Masood, F.; Yasin, T. Influence of sepiolite on thermal, mechanical and biodegradation properties of poly-3-hydroxybutyrate-co-3-hydroxyvalerate nanocomposites. *Appl. Clay Sci.* **2018**, *156*, 11–19.
- (19) Alkan, M.; Benlikaya, R. Poly(vinyl alcohol) nanocomposites with sepiolite and heat-treated sepiolites. *J. Appl. Polym. Sci.* **2009**, *112* (6), 3764–3774.
- (20) Nikolic, M. S.; Petrovic, R.; Veljovic, D.; Cosovic, V.; Stankovic, N.; Djonlagic, J. Effect of sepiolite organomodification on the performance of PCL/sepiolite nanocomposites. *Eur. Polym. J.* **2017**, *97*, 198–209.
- (21) Alvarez, A. Sepiolite: Properties and Uses. In *Developments in Sedimentology*; Singer, A.; Galan, E., Eds.; Elsevier, 1984; pp 253–287.
- (22) Kim, D. H.; Song, Y. S. Anisotropic optical film embedded with cellulose nanowhisker. *Carbohydr. Polym.* **2015**, *130*, 448–454.
- (23) Ahn, S. Y.; Song, Y. S. Viscoelastic characteristics of all cellulose suspension and nanocomposite. *Carbohydr. Polym.* **2016**, *151*, 119–129.